Molecular Plant
Research Article

CellPress
Partner Journal

The RING E3 ligase CLG1 targets GS3 for degradation via the endosome pathway to determine grain size in rice

Wensi Yang[1,4], Kun Wu[5], Bo Wang[1,4], Huanhuan Liu[1,4], Siyi Guo[1,4], Xiaoyu Guo[1,4], Wei Luo[1], Shengyuan Sun[2], Yidan Ouyang[2,3], Xiangdong Fu[5], Kang Chong[1,4,6], Qifa Zhang[3,*] and Yunyuan Xu[1,6,*]

[1]Key Laboratory of Plant Molecular Physiology, Institute of Botany, Chinese Academy of Sciences, Beijing 100093, China

[2]National Key Laboratory of Crop Genetic Improvement and National Centre of Plant Gene Research (Wuhan), Huazhong Agricultural University, Wuhan 430070, China

[3]National Key Laboratory of Crop Genetic Improvement and National Centre of Plant Gene Research (Wuhan), Hubei Hongshan Laboratory, Huazhong Agricultural University, Wuhan 430070, China

[4]University of Chinese Academy of Sciences, Beijing 100049, China

[5]The State Key Laboratory of Plant Cell and Chromosome Engineering, Institute of Genetics and Developmental Biology, Chinese Academy of Sciences, Beijing 100101, China

[6]Innovation Academy for Seed Design, CAS, Beijing 100101, China

***Correspondence: Qifa Zhang (qifazh@mail.hzau.edu.cn), Yunyuan Xu (xuyy@ibcas.ac.cn)**

https://doi.org/10.1016/j.molp.2021.06.027

ABSTRACT

G-protein signaling and ubiquitin-dependent degradation are both involved in grain development in rice, but how these pathways are coordinated in regulating this process is unknown. Here, we show that *Chang Li Geng 1* (*CLG1*), which encodes an E3 ligase, regulates grain size by targeting the Gγ protein GS3, a negative regulator of grain length, for degradation. Overexpression of *CLG1* led to increased grain length, while overexpression of mutated CLG1 with changes in three conserved amino acids decreased grain length. We found that CLG1 physically interacts with and ubiquitinats GS3which is subsequently degraded through the endosome degradation pathway, leading to increased grain size. Furthermore, we identified a critical SNP in the exon 3 of *CLG1* that is significantly associated with grain size variation in a core collection of cultivated rice. This SNP results in an amino acid substitution from Arg to Ser at position 163 of CLG1 that enhances the E3 ligase activity of CLG1 and thus increases rice grain size. Both the expression level of *CLG1* and the SNP CLG1^{163S} may be useful variations for manipulating grain size in rice.

Key words: grain size, *CLG1*, *GS3*, E3 ligase, endosome

Yang W., Wu K., Wang B., Liu H., Guo S., Guo X., Luo W., Sun S., Ouyang Y., Fu X., Chong K., Zhang Q., and Xu Y. (2021). The RING E3 ligase CLG1 targets GS3 for degradation via the endosome pathway to determine grain size in rice. Mol. Plant. **14**, 1699–1713.

INTRODUCTION

Rice is a staple food crop for half of the world's population. Grain size of rice is both a yield trait and quality trait and thus is one of the main breeding targets. Grain size is defined by the length, width, and thickness of the grain. Numerous QTLs controlling grain size, such as *GW2*, *GW5*, *GS3*, *DEP1*, and *GL3.1* (Fan et al., 2006; Song et al., 2007; Weng et al., 2008; Huang et al., 2009; Mao et al., 2010; Qi et al., 2012; Zhang et al., 2012; Ishimaru et al., 2013; Hu et al., 2015; Liu et al., 2017, 2018), have been identified in rice. Several signaling pathways regulating grain size have also been characterized, including the mitogen-activated protein kinase, G-protein, and ubiquitin-dependent signaling pathways.

In the ubiquitin-dependent pathway, E3 ligases are the key regulatory components, as they mediate substrate specificity (Morreale and Walden, 2016). In *Arabidopsis*, the ubiquitin receptor DA1 functions synergistically with the E3 ubiquitin ligases DA2 and BB/EOD1 to target different substrates and

Published by the Molecular Plant Shanghai Editorial Office in association with Cell Press, an imprint of Elsevier Inc., on behalf of CSPB and CEMPS, CAS.

regulate grain size (Li et al., 2008; Xia et al., 2013). In rice, the RING (Real Interesting New Gene)-type E3 ligase GW2 ubiquitinates EXPANSIN-LIKE 1 and negatively regulates seed size (Choi et al., 2018). GW2 also targets the glutaredoxin protein WG1, which acts upstream of OsbZIP47 in the control of grain width and weight, for degradation (Hao et al., 2021). Ubiquitin regulates protein transport between membrane compartments by serving as a sorting signal on protein cargo and by controlling the activity of the trafficking machinery (Hicke and Dunn, 2003). One example is the sorting of proteins with K63-linked ubiquitin chains by multivesicular bodies for degradation by the endosome degradation pathway (Lauwers et al., 2009). However, little is known about how the endosome degradation pathway controls grain size in rice.

G-protein signaling plays an important role in controlling grain size and shape in rice (Xu et al., 2019). The G-protein complex is responsible for coupling many cell surface G-protein-linked receptors with the appropriate intracellular effectors. The receptors are activated by ligands, and the effectors mediate various cellular responses. The heterotrimeric G-protein complex consists of the Gα, Gβ, and Gγ subunits. The rice genome encodes two typical Gγ proteins, RGG1 and RGG2, and three atypical members, GGC2, DEP1, and GS3 (Xu et al., 2016; Liu et al., 2018; Sun et al., 2018). *GS3* is a major negative regulator of grain length (Fan et al., 2006; Mao et al., 2010). It genetically interacts with *GL3.3*, which encodes a GSK3/SHAGGY-like kinase, and the *gs3 gl3.3* double mutant produces extra-long grains (Xia et al., 2018). Both GS3 and DEP1 interact with OsMADS1, enhancing its transcriptional activity and thus regulating grain size and shape (Liu et al., 2018). However, the relationship between the various pathways involved in grain size regulation is largely unknown.

Here, we identified a gain-of-function mutant, *Chang Li Geng1-1* (*clg1-1*), that exhibits increased grain size. *CLG1* was predicted to encode an E3 ligase containing a CHY zinc-finger domain and a C3H2C3-type RING domain (Kobayashi et al., 2013). Consistent with the gain-of-function mutant phenotype, overexpression of *CLG1* led to increased grain size. We showed that CLG1 regulated grain size by directly interacting with GS3. The full-length GS3 protein (GS3-2) could be ubiquitinated by CLG1 and degraded via the endosome degradation pathway. However, a truncated GS3 protein (GS3-4) could not be endocytosed and accumulated on the membrane, which inhibited G-protein signaling and resulted in short grains. The substitution of Ser163 for Arg163 in a natural population enhanced CLG1 activity. Our work reveals a connection between the ubiquitin endosome degradation pathway and G-protein signaling in grain size regulation.

RESULTS

Identification of *CLG1* as a positive regulator of grain size

The *clg1-1* mutant was obtained from a tissue culture seedling population generated by *Agrobacterium tumefaciens*-mediated transformation of Zhonghua 10 (ZH10, *Oryza sativa* L. ssp. *japonica/geng*). The brown rice grain length of *clg1-1* (6.1 ± 0.05 mm) was ~21% higher compared with that of the wild-type ZH10 (5.0 ± 0.03 mm) (Figure 1A). Genomic DNA sequencing showed that the T-DNA was inserted in the *Os05g47770* gene (Supplemental Figure 1A and 1B). However, a knockout mutant of *Os05g47770* generated by CRISPR/Cas9 technology did not show any changes in grain length compared with the wild type (Supplemental Figure 1C and 1D).

We thus cloned the gene based on the grain length trait. A mapping population was generated by crossing *clg1-1* with GLA4 (Guanglu Ai 4), an *indica/xian* variety with a seed size similar to that of ZH10. Using 4600 F_2 plants, we mapped the *CLG1* locus to a 5 Mb region on the long arm of chromosome 5 between the molecular markers RM3809 and RM334; this region was further narrowed down to 128 kb between markers CL12 and CL15 (Figure 1B). Informatic analysis identified 16 putative genes in this region (Supplemental Table 1). The transcription levels of these genes in young panicles (10 ± 1 cm in length) were determined by qRT–PCR. The transcript level of *Os05g47780* in the *clg1-1* mutant was about four times that in the wild type; the reason why transcription levels are higher in the mutant is not clear (Supplemental Figure 2A). *Os05g47780* encodes the E3 ligase OsHRZ2 (*Oryza sativa* Hemerythrin motif-containing RING- and Zn-finger protein 2) (Figure 1C), which was reported to regulate iron acquisition (Kobayashi et al., 2013; Selote et al., 2015). Considering the reported involvement of E3 ubiquitin ligases in seed size regulation (Song et al., 2007; Xia et al., 2013) and the highly elevated expression of *Os05g47780* in panicles (Supplemental Figure 2A), we considered *Os05g47780* as the candidate for *CLG1*.

To verify the above speculation, the following transgenic rice plants were generated: *CLG1* overexpression lines (OEs) and *CLG1* knockout lines (KOs) in the ZH10 background. All of these transgenic plants were confirmed by qRT–PCR (Supplemental Figure 2B). The two *CLG1* KOs, KO1 and KO2, were generated by CRISPR/Cas9, and both of these lines contained frameshift mutations (Figure 1D). The OEs (OE1 and OE2) showed significantly increased grain length compared with ZH10 (Figure 1E), while the grain lengths of KO1 and KO2 plants were not significantly different from that of ZH10. We also used CRISPR/Cas9 to knock out the *Os05g47780* gene in the *clg1-1* background (the resulting lines are referred to as complementation lines [COMs]). The grains of COM1 and COM2 were obviously shorter than those of *clg1-1* (Figure 1F and 1G). These data suggested that *clg1-1* is a gain-of-function mutant of *Os05g47780* and that the *CLG1* gene positively regulates grain length.

CLG1 encodes a RING E3 ligase

E3s are the most heterogeneous class of enzymes in the ubiquitination pathway. The RING-type E3 ubiquitin ligases comprise the largest class of E3s (Morreale and Walden, 2016). RING E3 ligases serve as a scaffold mediating the direct transfer of ubiquitin to the substrate, and can function as monomers, homodimers, heterodimers, or even as multiple subunits. RING domain E3 ligases are required for many cellular processes (Gao et al., 2011; Park et al., 2012; Hu et al., 2013; Ding et al., 2015; Lim et al., 2015; Yang et al., 2015, 2016; Liu et al., 2016; You et al., 2016).

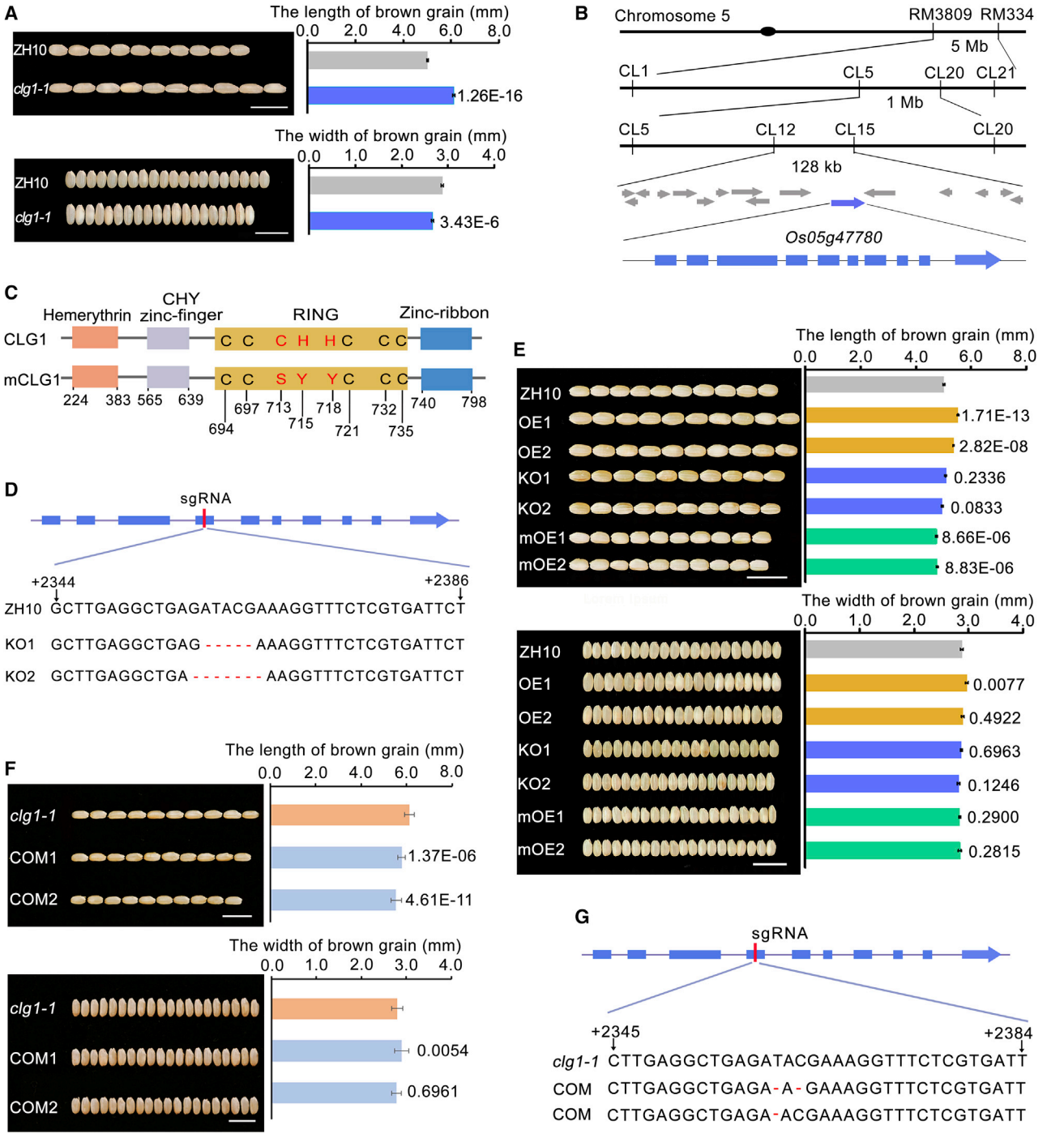

Figure 1. Map-based cloning of *CLG1*.

(A) The length and width of brown rice grains of wild-type Zhonghua 10 (ZH10) and mutant *clg1-1*. Scale bars correspond to 1 cm. Values are given as means ± SE (n = 30). The P values are from Student's t-tests between the wild type and mutant.

(B) Genetic map developed using 4600 segregating F_2 plants. The mutant *clg1-1* was crossed with GLA4, an *indica/xian* variety.

(C) A diagram of wild-type CLG1 and mutated CLG1 (mCLG1). The key residues for Zn^{2+} ion chelation in the RING domain of CLG1, Cys^{713}, His^{715}, and His^{718}, were mutated to Ser^{713}, Tyr^{715}, and Tyr^{718} residues, respectively.

(D) The mutation sites in the *CLG1* gene in the knockout mutant 1 (KO1) and KO2 generated by CRISPR/Cas9.

(E) The length and width of brown rice grains of wild-type ZH10 and homozygous transgenic plants. Scale bars correspond to 1 cm. OE1 and OE2 indicate *CLG1*-overexpressing plants. KO1 and KO2 indicate the two KOs in the ZH10 background, generated using CRISPR/Cas9. mOE1 and mOE2 indicate *mCLG1* overexpression lines. Values are given as means ± SE (n = 30). Student's t-test was used to generate the P values.

(F) The length and width of brown rice grains of *Os05g47780* KOs in the *clg1-1* mutant background. Values are given as means ± SE (n = 30). Student's t-test was used to generate the P values.

(G) The mutation sites in *Os05g47780* in the *clg1-1* mutant lines generated by CRISPR/Cas9. See also supplemental Figures 1 and 2.

The *CLG1* gene was predicted to contain an open reading frame with 10 exons and 9 introns, encoding an E3 ligase of 811 amino acids with 4 domains: a hemerythrin domain, a CHY zinc-finger domain, a RING domain, and a zinc-ribbon domain (Figure 1C). The hemerythrin domain is involved in the regulation of iron acquisition (Kobayashi et al., 2013; Aung et al., 2018), and the CHY zinc-finger domain includes a conserved CxHY motif. The RING domain is a C3H2C3-type zinc finger, in which the Cys^{713}, His^{715}, and His^{718} residues are involved in the chelation of two Zn^{2+} ions and are required for E3 ligase activity (Supplemental Figure 3A) (Freemont et al., 1991; Stone et al., 2005; Ding et al., 2015). BLAST searches of protein databases identified a number of orthologous proteins of CLG1 in various higher plants. In addition, a phylogenetic tree of CLG1 proteins from selected monocot and dicot species showed that CLG1 was evolutionarily most closely related to orthologs in *Oryza brachyantha* (OB05G32390), *Brachypodium distachyon* (BRADI_2g18270v3), and *Aegilops tauschii* (LOC109731892) (Supplemental Figure 3B). Some of the orthologous proteins of CLG1 have been confirmed to be E3 ligases (Selote et al., 2018).

To test CLG1 for E3 ligase activity, we performed an *in vitro* ubiquitination assay using a purified Maltose-Binding Protein (MBP):CLG1 fusion protein incubated with purified E1, E2, and ubiquitin following an established method (Zhang et al., 2007). The reaction products were analyzed by immunoblotting using an anti-ubiquitin antibody. A smeared higher-molecular-mass band was detected in the reactions containing MBP:CLG1 incubated with purified E1, E2, and ubiquitin, but not in those lacking E1, E2, or ubiquitin (Supplemental Figure 3C). These western blotting data clearly showed that CLG1 has E3 ligase activity and can mediate self-ubiquitination *in vitro*.

A previous study showed that chelation of a Zn^{2+} ion by one Cys and two His residues in the RING domain is necessary for the activity of RING-type E3 ligases (Stone et al., 2005; Ding et al., 2015). The substitution of key amino acids in the RING motif is a common strategy used to produce dominant negative mutants of E3 proteins (Xie et al., 2002; Zhang et al., 2005; Dong et al., 2006; Koiwai et al., 2007; Peng et al., 2013; Jung et al., 2015). We generated a mutated form of CLG1 (mCLG1) by substituting the three key amino acids Cys^{713}, His^{715}, and His^{718} with Ser^{713}, Tyr^{715}, and Tyr^{718}, respectively (Figure 1C). A ubiquitination assay showed that mCLG1 had no ligase activity (Supplemental Figure 3C). We also generated *mCLG1*-overexpressing rice plants (mOEs), which showed significantly decreased grain length compared with wild type (Figure 1E). These results suggested that the inactivated mCLG1 may competitively interact with the substrate and thus decrease the ubiquitination of substrates by the endogenous wild-type CLG1 protein. Therefore, the E3 activity of CLG1 is essential for CLG1 genetic function.

CLG1 physically interacts with GS3

The results from phenotypic analysis of transgenic plants and assays of the E3 ligase activity of CLG1 and mCLG1 implied that CLG1-mediated protein degradation may affect grain size. Thus, we speculated that the candidate target protein of CLG1 could be a negative regulator of grain length. We thus investigated the interactions of CLG1 with known negative regulators of seed size, GL3.1, GSK2, TGW6, GS5, GW5, and GS3, using the yeast two-hybrid (Y2H) system (Figure 2A). GS3 (Os03g0407400), which negatively regulates grain size and organ size by competitively interacting with Gβ (Fan et al., 2006; Mao et al., 2010; Sun et al., 2018), was identified as a CLG1-interacting partner. However, no interaction was detected between CLG1 and DEP1/dep1 (a truncated DEP1 protein with a short tail), another Gγ protein in rice that interacts with Gβ (Figure 2A).

The GS3 protein has three domains, the N-terminal organ size regulation domain (amino acids 12–72), the middle region (73–114), and the C-terminal Cys-rich domain referred to as the "tail" (115–232) (Figure 2B) (Mao et al., 2010; Botella, 2012; Sun et al., 2018). Four alleles of *GS3* were previously identified: *GS3-1* (Zhenshan 97), *GS3-2* (Nipponbare and ZH10), *GS3-3* (Minghui 63), and *GS3-4* (Chuan 7). GS3-1 and GS3-2 differ by only one amino acid in the C-terminal region and have the same effect on grain length. *GS3-3* from Minghui 63 has an SNP causing premature termination of the predicted protein, resulting in loss of the functional domain and thus the production of long grains. *GS3-4* from Chuan 7 has a 1-bp deletion at 357 bp, which causes a frameshift in the C terminus, yielding a truncated 149 amino acid protein (Mao et al., 2010; Sun et al., 2018).

The interaction between CLG1 and the full-length GS3-2 protein from ZH10 was confirmed by a pull-down assay. The glutathione S-transferase (GST):CLG1 and MBP:GS3-2 fusion proteins were expressed in *Escherichia coli* and purified by affinity chromatography. GST:CLG1 was able to pull down MBP:GS3-2 but not MBP, which suggested that CLG1 interacts directly with GS3-2 (Figure 2C). The interaction between CLG1 and GS3-2 was also demonstrated using the split firefly luciferase complementation assay in *Nicotiana benthamiana* leaf cells and bimolecular fluorescence complementation (BiFC) assay in rice protoplasts (Figure 2D and 2E). The Y2H and BiFC results showed that CLG1 could interact with GS3-1, GS3-2, and GS3-4, but not GS3-3 (Figure 2A and 2E). GS3-3 is the shortest of the GS3 proteins, containing only the N-terminal 55 amino acids (Figure 2B), suggesting that this region does not interact with CLG1. Like CLG1, mCLG1 could interact with GS3-1, GS3-2, and GS3-4 (Supplemental Figure 4), which suggested that the mutation in the RING domain did not affect the interaction between CLG1 and GS3.

To search for the CLG1 target site in GS3, various truncated forms of GS3-2 were used as baits and the full-length sequence of CLG1 as the prey in Y2H assays. We designated the truncated forms obtained by deletions of the N-terminal 1–65, 1–114, and 68–232 amino acids as GS3-2Δ1–65, GS3-2Δ1–114, and GS3-2Δ68–232, respectively (Figure 2B). Deletion of amino acids 1–65 did not affect the interaction between GS3-2Δ1–65 and CLG1 in the Y2H assay. GS3-2Δ1–114 and GS3-2Δ68–232, which lacked the middle region, could not interact with CLG1 (Figure 2A). Thus amino acids 66–114 in the middle region of GS3-2 are necessary for the interaction between GS3-2 and CLG1.

CLG1 ubiquitinates GS3 on the tail domain and targets it for endosomal degradation

Confocal microscopic observation showed that both GS3-1 and GS3-2 interacted with CLG1 in the cytomembrane and

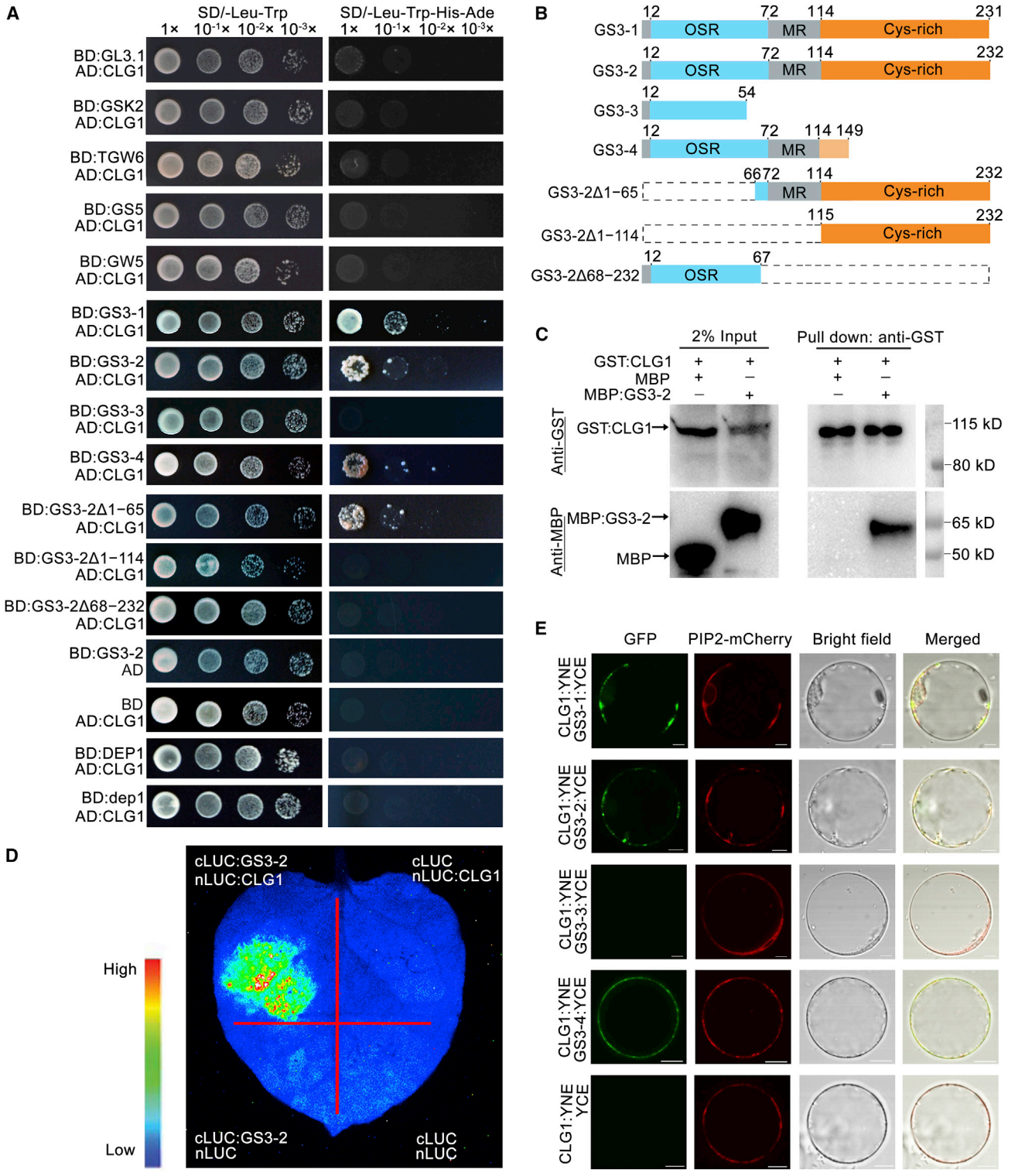

Figure 2. The interaction between CLG1 and GS3.

(A) GAL4-based Y2H assay showing that CLG1 interacts with GS3-2 and other proteins related to grain size. AD, activation domain; BD, binding domain; SD, synthetic dropout.

(B) The proteins encoded by different alleles of *GS3* and the deletion constructs of *GS3-2*. OSR, organ size regulation domain; MR, middle region.

(C) Pull-down assay showing the interaction between GST:CLG1 and MBP:GS3-2.

(D) Split luciferase complementation indicates an *in vivo* interaction between CLG1 and GS3-2.

(E) Verification of the interaction between CLG1 and GS3 proteins by BiFC in rice protoplasts. PIP2 is a membrane-localized marker. Scale bars correspond to 10 μm.

cytoplasm, but interaction of GS3-4 with CLG1 only occurred on the cytomembrane (Figure 2E). It was reported that PYR1/PYL membrane proteins modified by K63-linked ubiquitin can be degraded by the endosome degradation pathway (Yu et al., 2016), which led us to speculate that ubiquitinated GS3 may also be sorted into lysosomes/vacuoles for degradation via the endosome-mediated pathway. To test this, the localization of GS3-2 and GS3-4 was observed in *N. benthamiana* leaf cells (Figure 3A and 3B). Confocal imaging showed that GS3-2, but not GS3-4, was colocalized with the early endosome marker OsSCAMP1 (Lam et al., 2007) and the late endosome marker ARA7 (Spitzer et al., 2006). Live-cell time-lapse imaging showed that GS3-2:GFP was distributed as discontinuous fluorescent spots on the membrane and in the cytoplasm. The fluorescence intensity of GS3-2:GFP obviously decreased from 5 to 7 h after cycloheximide (CHX) (an efficient inhibitor of eukaryotic protein synthesis) treatment, whereas the signal of GS3-4:GFP on the membrane did not (Supplemental Figure 5 and Figure 3C). When mCLG1 was overexpressed in *N. benthamiana* leaf cells, more GS3-2:GFP accumulated in the cytomembrane than when CLG1 was overexpressed (Figure 3C and Supplemental Figure 6). To further verify the trafficking of GS3-2 from the membrane to cytoplasm, we employed the protein cargo transportation inhibitor wortmannin (WM), which results in the formation of enlarged multivesicular bodies (Robinson et al., 2008), with *Arabidopsis* VPS23A, a member of the endosomal sorting complex required for transport-mediated sorting, as a marker (Yu et al., 2016). Under WM treatment, cells co-expressing GS3-2:GFP and VPS23A:mCherry displayed more punctate fluorescent signals than those without WM treatment (Supplemental Figure 7 and Figure 3D). To detect the ubiquitination of GS3 *in vivo*, Myc:GS3-2 and Myc:GS3-4 were expressed in *N. benthamiana* leaves. Western blot analysis with an anti-ubiquitin antibody showed that both Myc:GS3-2 and Myc:GS3-4 were ubiquitinated, and that the ubiquitination level of Myc:GS3-2 was higher than that of Myc:GS3-4 (Supplemental Figure 8). These results suggested that the ubiquitinated GS3-2 protein could be sorted into the lysosome/vacuole for degradation, and that ubiquitinated GS3-4 lacking the Cys-rich tail could not be sorted into the endosome and thus accumulated on the membrane.

The different distributions of GS3-2 and GS3-4 and the physical interactions of CLG1 with GS3-1, GS3-2, and GS3-4 suggested that these GS3 proteins may differ in ubiquitination by the E3 ligase CLG1. Moreover, in our previous work, *Ubi::GS3-1:Flag* (GS3-1F) transgenic plants showed reduced grain length compared with the wild type, and *Ubi::GS3-4:Flag* (GS3-4F) transgenic plants produced even shorter grains. The shorter grain length of GS3-4F compared with GS3-1F is due to the higher accumulation of GS3-4 because of its failure to be degraded (Sun et al., 2018).

To identify differences in ubiquitination between GS3-2 and GS3-4, ubiquitination sites were predicted by Musite (Qiu et al., 2019). Six sites (K10, K76, K87, K88, K126, and K153) were identified in GS3-2, and four sites (K10, K76, K87, and K88) in GS3-4. We performed *in vitro* ubiquitination reactions, in which either the GST:GS3-2:Myc or GST:GS3-4:Myc fusion protein was used as the substrate and the recombinant protein MBP:CLG1 was used as the E3 ligase. In the presence of E1, E2, and ubiquitin, smeared higher-molecular-mass bands could be detected by the anti-ubiquitin antibody and anti-K63-linked ubiquitin antibody. The band intensity decreased with decreasing amounts of GST:GS3-2:Myc or GST:GS3-4:Myc (Figure 4A). When the ubiquitin was substituted by ubiquitin^{K63R}, the ubiquitination levels of GS3-2 and GS3-4 obviously decreased and the K63-linked form could not be detected (Figure 4B). These results suggested that CLG1 mediates K63-linked polyubiquitination of GS3-2 and GS3-4.

The products of *in vitro* ubiquitination reactions were also detected by liquid chromatography-mass spectrometry (LC-MS). The LC-MS assay revealed ubiquitination of K76, K87, K88, and K153 in GS3-2, while only K76 and K88 in GS3-4 were found to be ubiquitinated (Figure 4C). Thus, CLG1 targets and ubiquitinates the middle region of both the full-length form GS3-2 and the truncated form GS3-4. We inferred that the lack of K153 in GS3-4 (149 amino acids in length) might be the main reason why GS3-4 could not be degraded by the endosome degradation pathway. This provided an explanation for the over-accumulation of GS3-4 protein observed previously (Sun et al., 2018), which had a large effect on grain size.

To investigate the degradation efficiency of the full-length variant GS3-1 and truncated variant GS3-4 by the endosome degradation pathway, 14-day-old seedlings of *Ubi::GS3-1:Flag* and *Ubi::GS3-4:Flag* transgenic rice were treated with CHX, with or without E64d (an inhibitor of vacuolar/lysosomal hydrolases). Western blotting showed that E64d could obviously suppress GS3-1:Flag degradation after treatment for 2, 4, and 6 h. However, levels of GS3-4:Flag remained similar with or without E64d treatment (Figure 4D). These results suggest that GS3-1 degradation may be partially mediated by the endosome degradation pathway.

To test the relationship between CLG1 and GS3 *in vivo*, *Ubi::CLG1* was transformed into a *Ubi::GS3-1:Flag*-overexpressing line (GS3-1F) and a *Ubi::GS3-4:Flag*-overexpressing line (GS3-4F); the resulting lines were designated CLG1-OE/GS3-1F and CLG1-OE/GS3-4F, respectively. More than three independent transgenic plants were obtained in each background (Supplemental Figure 9B). The protein levels of GS3-1:Flag and GS3-4:Flag were detected using an antibody against Flag. Compared with GS3-1F, the two CLG1-OE/GS3-1F transgenic plants showed lower levels of GS3-1:Flag (0.72 and 0.32 relative to GS3-1F). In contrast, the levels of GS3-4:Flag in CLG1-OE/GS3-4F transgenic plants were reduced to a much lesser extent (0.87, 0.82, and 0.89 relative to GS3-4F) (Figure 4E). Furthermore, the CLG1-OE/GS3-1F transgenic plants showed significantly increased grain length compared with GS3-1F, and the grain lengths of CLG1-OE/GS3-4F transgenic plants were not significantly different from those of GS3-4F (Supplemental Figure 9A). These results suggested that overexpression of *CLG1* enhances degradation of GS3-1 *in vivo*, but does not much enhance that of GS3-4.

Natural variation at the *CLG1* locus affects grain length

To investigate the possible effect of natural variation in *CLG1* on grain length, the sequences of 346 accessions of cultivated rice from the 3000 Rice Genome Project were analyzed (https://snp-seek.irri.org). Using the NIP sequence (rice.plantbiology.msu.edu) as the reference, 14 SNPs were identified at the *CLG1* locus

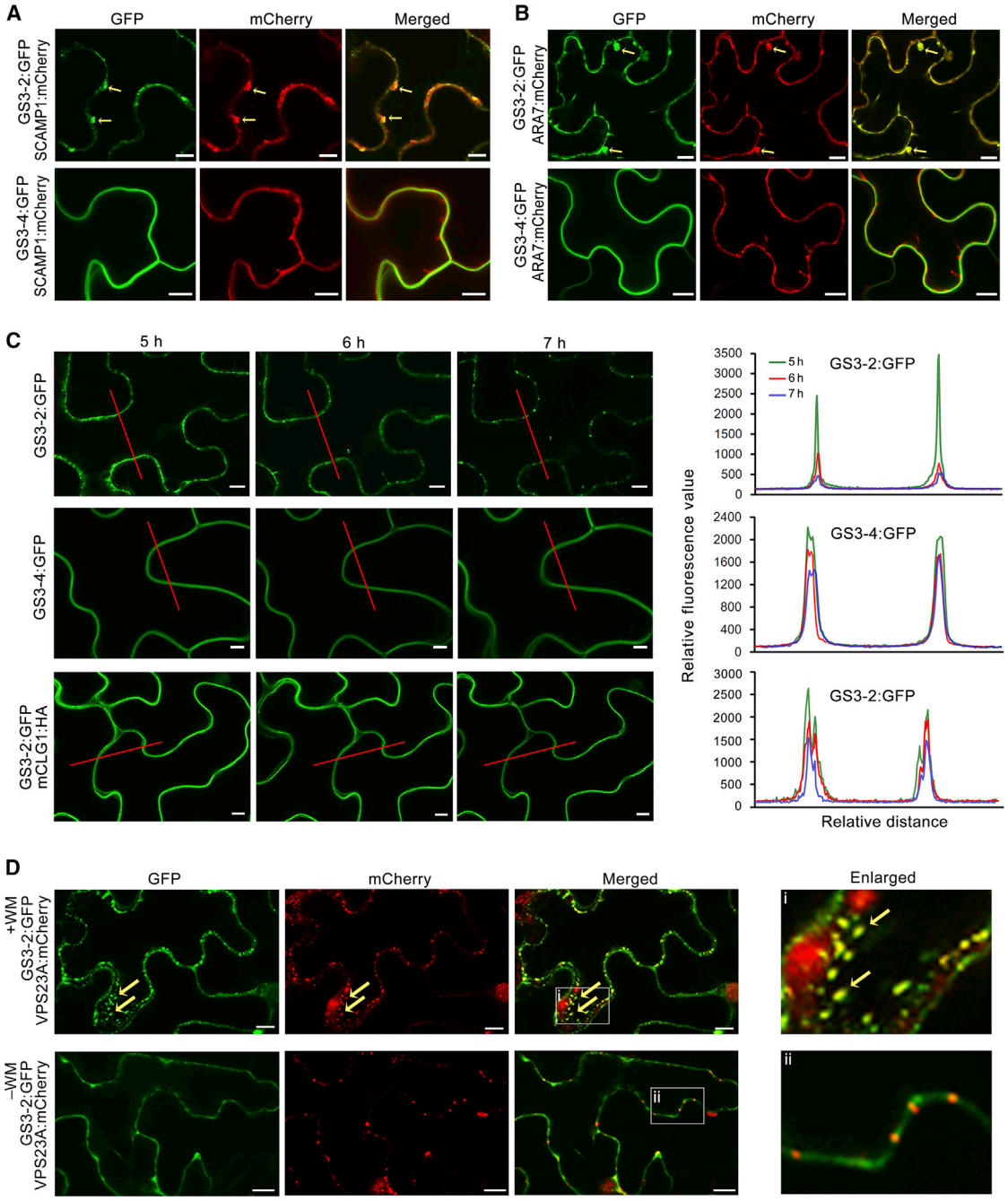

Figure 3. Subcellular localization of GS3-2 and GS3-4.

(A) GS3-2 partially localizes to the early endosomes. GS3-2:GFP or GS3-4:GFP was transiently co-expressed with the early endosome marker OsSCAMP1:mCherry in *N. benthamiana* leaves using agroinfiltration. After 3 days, the resulting fluorescence was observed by confocal laser scanning microscopy. Arrows indicate the overlap of green and red fluorescence. Scale bars correspond to 10 μm.

(B) GS3-2 partially localizes to the late endosomes. GS3-2:GFP or GS3-4:GFP was co-expressed with the late endosome marker ARA7:mCherry in *N. benthamiana* leaves using agroinfiltration. After 3 days, the resulting fluorescence was observed by confocal laser scanning microscopy. Scale bars correspond to 10 μm.

(C) The dynamic distribution of GS3-2 and GS3-4 in the plasma membrane from 5 to 7 h after cycloheximide (CHX) treatment. The fluorescence intensity of the labeled area with the red line was determined using the ImageJ plot profile tool. CHX, actidione; y axes are relative pixel intensity. Scale bars correspond to 10 μm.

(D) Trafficking of GS3-2 and VPS23A from membrane to vacuole. GS3-2:GFP and the late endosome marker VPS23A:mCherry were co-expressed in *N. benthamiana* leaves using agroinfiltration. Treatment with the protein cargo transportation inhibitor wortmannin (WM) blocked protein cargo trafficking to vacuoles and resulted in the formation of enlarged multivesicular bodies. The boxed areas are enlarged on the right. Scale bars correspond to 10 μm.

(from −2736 to +4733) (Figure 5A). Using these SNPs, the accessions could be divided into four haplotypes. Three haplotypes (Hap2, Hap3, and Hap4) were found in *indica/xian* accessions, two (Hap1 and Hap4) were found in temperate *japonica/geng* accessions, and two (Hap2 and Hap4) in tropical *japonica/geng* accessions. Only one SNP (27878401) in the open reading frame caused amino acid variation; 27878401A, which occurred only in Hap1, encoded Arg^{163}, and 27878401T in Hap2, Hap3, and Hap4 encoded Ser^{163}. Accessions having Hap2, Hap3, and Hap4 had longer grains than those having Hap1 (27878401A) (Figure 5B). These results indicated that SNP 27878401T increases grain length. Although Hap2, Hap3, and Hap4 had the same coding sequence, accessions with Hap4 obviously produced longer grains than those with the other haplotypes in the group of 122 *indica/xian* accessions (Figure 5C) and in the 78 temperate *japonica/geng* accessions (Figure 5D).

To exclude the possibility that different alleles of *GS3* have different effects on grain length, the 166 accessions that carried the *GS3-1/-2* alleles were selected and their grain lengths were compared. The statistical data showed that accessions with these three haplotypes had similar grain lengths in the *GS3-1/-2* background (Figure 5E).

Hap1 and Hap3 showed the largest difference in terms of the number of SNPs among the four haplotypes, in addition to SNP 27878401T/A, which causes an amino acid substitution. We thus compared the effects of Hap1 and Hap3 on grain length and weight. A chromosome segment substitution line (CSSL), $93\text{-}11^{Hap1}$ (*CLG1*^{Hap1}*/GS3-3*), which carried the *CLG1*^{Hap1} allele from NIP and the *GS3-3* allele from the *indica/xian* cultivar 93-11, showed no significant difference compared with 93-11 (*CLG1*^{Hap3}*/GS3-3*). However, the CSSL NIP^{Hap3} (*CLG1*^{Hap3}*/GS3-2*), which carried *CLG1*^{Hap3} from 93-11 and the *GS3-2* allele from NIP, produced longer grains than NIP (*CLG1*^{Hap1}*/GS3-2*) (Figure 5F). Thus *CLG1*^{Hap3} could increase grain length depending on the allele at the *GS3* locus. These results suggested that the *CLG1* locus may play a role in grain size regulation at the species level.

The E3 ligase activity of $CLG1^{163S}$ is stronger than that of $CLG1^{163R}$

We speculated that Hap2, Hap3, and Hap4 of *CLG1* may encode proteins with higher E3 ligase activity than that encoded by Hap1, such that GS3-2 may be more readily ubiquitinated by $CLG1^{163S}$ than $CLG1^{163R}$. To test this hypothesis, we performed an *in vitro* ubiquitination assay, comparing the purified MBP:$CLG1^{163S}$ fusion protein against MBP:$CLG1^{163R}$. Western blotting showed that the mass of ubiquitinated-MBP:$CLG1^{163S}$ was much higher than that of MBP:$CLG1^{163R}$ (Figure 6A). These results suggested that $CLG1^{163S}$ has much higher E3 ligase activity than MBP:$CLG1^{163R}$.

DISCUSSION

CLG1 regulates grain length through G-protein signaling

GS3 is the first cloned quantitative trait locus gene that negatively regulates grain size and organ size (Fan et al., 2006; Mao et al., 2010). Previous work showed that GS3 and DEP1/GGC2 competitively interact with RGB1 in the G-protein signaling pathway, and that the C-terminal tail of GS3 is necessary for its degradation. The C-terminal tail-mediated self-degradation of GS3 is critical for the strength of G-protein signaling in grain size regulation (Sun et al., 2018).

In this study, we showed that CLG1, an E3 ubiquitin ligase, can interact with GS3 for its degradation to regulate G-protein signaling. CLG1 functions in endocytosis-mediated degradation instead of 26 proteasome-mediated degradation and regulates grain size through the G-protein signaling pathway (Figure 6B). The rate of GS3 degradation determines the balance between the Gα-Gβ-GS3 and Gα-Gβ-DEP1/GGC2 complexes to regulate grain length. CLG1 targets GS3 for degradation mainly through the ubiquitination of GS3's C-terminal tail. In the gain-of-function mutant *clg1-1*, the increased amount of CLG1 enhances degradation of GS3 and thus reduces its binding of Gβ, leading to an increase in grain length. In the GS3-2 protein, ubiquitination of the C-terminal tail by CLG1 targets it for degradation, which releases Gβ from GS3, allowing DEP1 and GGC2 to bind to Gβ and resulting in the production of medium-length grains. In contrast, the absence of a C-terminal tail in GS3-4 greatly reduces ubiquitination by CLG1 and results in the accumulation of GS3-4, most of which binds Gβ and prevents the binding of DEP1 and GGC2, leading to the production of short grains. GS3-3 contains only the N-terminal 55 amino acids and cannot bind to Gβ, which causes Gβ to be completely bound by DEP1 or GGC2, and the resulting enhancement of G-protein signaling results in the production of long grains. This working model explains the function of the E3 ligase CLG1 and updates our previous understanding of grain size regulation by the Gγ proteins DEP1/GGC2 and GS3 (Sun et al., 2018).

CLG1 ubiquitinates GS3, resulting in endosomal sorting and vacuolar degradation

Ubiquitin/26S proteasome-dependent protein degradation is involved in many cellular processes. However, little is known about the role of the ubiquitin/endosome-mediated degradation pathway in regulating plant development. WTG1/OsOTUB1, an otubain-like protease with deubiquitination activity, controls grain size by regulating cell size (Huang et al., 2017). OsOTUB1 can interact with IPA1/OsSPL14 to inhibit its K63-ubiquitination but promote its K48-polyubiquitination, thereby resulting in degradation of IPA1/OsSPL14 through the proteasome pathway (Wang et al., 2017). Our data suggested that the E3 ligase CLG1 determines grain size by ubiquitinating the Gγ subunit GS3 and targeting it for endosomal degradation. The full-length variants GS3-1 and GS3-2 interacted with CLG1 in both the cytoplasm and cytomembrane, but the interaction of CLG1 with the truncated variant GS3-4 was limited by the subcellular localization of GS3-4, which is only found on the cytomembrane (Figure 2). Our results also suggested that CLG1 is involved in endosome sorting and vacuolar degradation, a process in which ubiquitination is known to be essential (Raiborg and Stenmark, 2009). Considering the differences in the subcellular localization of GS3-2 and GS3-4 (Figure 3) and the lack of a Cys-rich tail in GS3-4 (Figure 2), we speculate that ubiquitination on the C-terminal tail acts as a label for GS3 endocytosis. GS3-4 lacks the ubiquitin label and thus accumulates in the cytomembrane, whereas GS3-2 labeled by CLG1

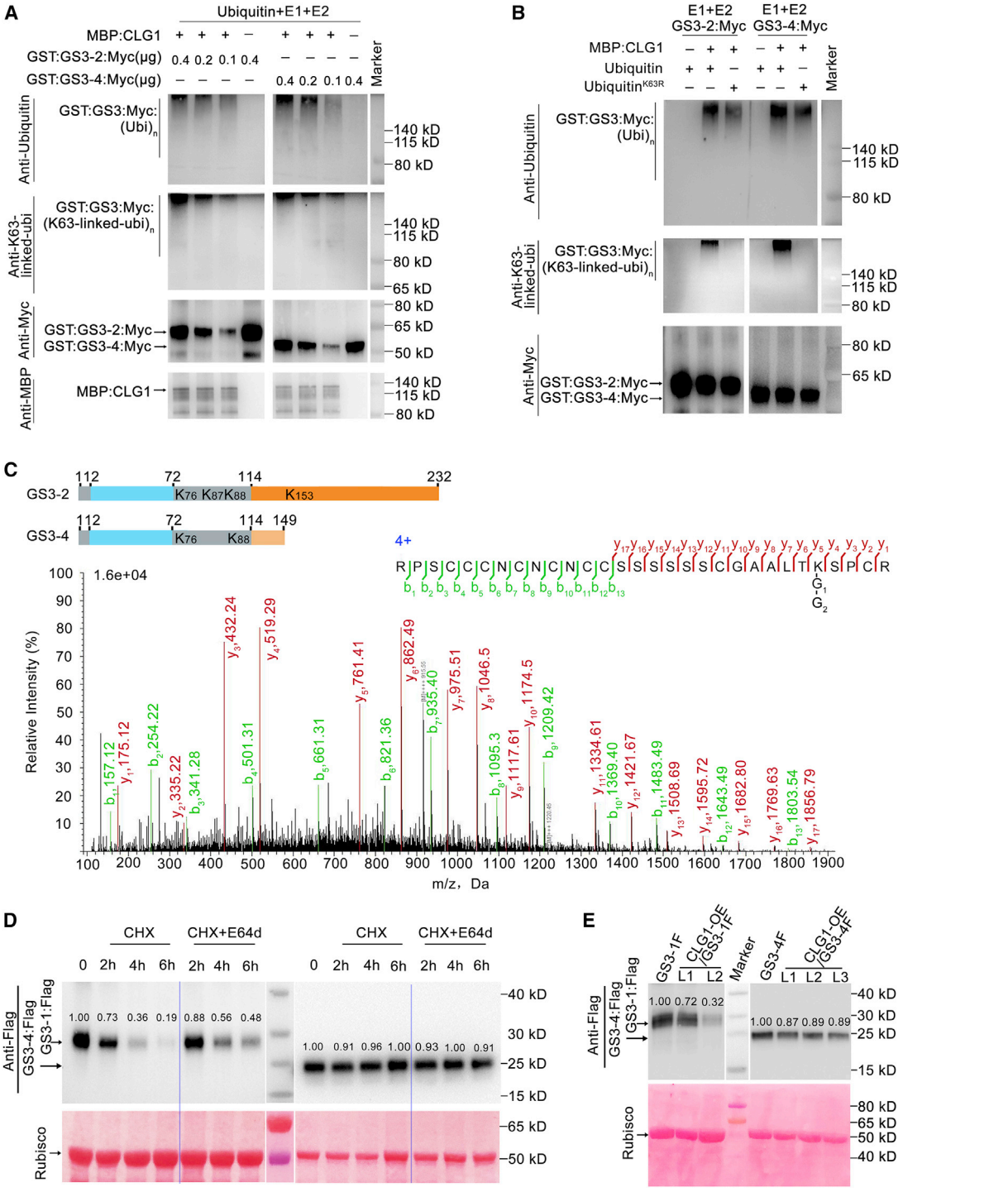

Figure 4. Identification of GS3 as a substrate of CLG1.

(A) Ubiquitination of GS3-1 and GS3-4 by CLG1 *in vitro*. "+" and "−" indicate the presence and absence of the components in each reaction mixture, respectively. Ubiquitinated GST:GS3-2:Myc and GST:GS3-4:Myc were detected with anti-ubiquitin and anti-K63-linked-ubiquitin antibodies. Immunoblots hybridized with anti-Myc and anti-MBP antibodies were used as a loading control.

(B) The K63-linked ubiquitination of GS3-1 and GS3-4 by CLG1 *in vitro*. "+" and "−" indicate the presence and absence of the components in each reaction mixture, respectively. Ubiquitinated fusion proteins GST:GS3-1:Myc and GST:GS3-4:Myc were detected with anti-ubiquitin and anti-K63-linked-ubiquitin antibodies. Western blotting with anti-Myc was performed as a loading control.

(C) Identification of ubiquitination sites in GS3-2 and GS3-4 using liquid chromatography-mass spectrometry (LC-MS). Different colors represent different domains. The Lys (K) residues marked with numbers, which were identified by LC-MS, could be ubiquitinated by CLG1 *in vitro*. K153 in the GS3-2 peptide

(legend continued on next page)

can be sorted into lysosomes/vacuoles for degradation, releasing the inhibition of G-protein signaling.

Natural variation in *CLG1* regulates grain length

Many studies have shown that natural variation in regulatory regions affecting gene expression level is an important source of grain size variation. For example, a single SNP in the promoter of *TGW2* causes variation in the expression level of the gene to regulate seed size by restraining cell division (Ruan et al., 2020). Similarly, two natural SNPs in the *GS5* promoter are responsible for its higher transcript level in a wide-grain variety and lower level in a narrow-grain variety (Xu et al., 2015). The tandem duplication of *GL7* led to its upregulation and an increase in grain length (Wang et al., 2015b). A 10-bp deletion in the promoter of *GW8*/*SPL16* results in downregulation of *GW7* and the production of slender grains (Wang et al., 2012, 2015a). Mutation of the OsmiR396c target site in the *GL2*/*GS2*/*OsGRF4* gene elevates its transcript level and increases grain size (Che et al., 2015; Hu et al., 2015). Our results show that the enhanced expression of *CLG1* in the *clg1-1* mutant causes long grains.

Structural changes in the coding sequence altering protein activity also provide important sources of grain size variation. The truncated GS3 variant GS3-3, which has only 55 amino acids and complete loss of function, causes the production of longer grains in rice (Sun et al., 2018). C-terminal truncation of OsMADS1 (OsMADS1^{lgy3}) leads to a slender grain (Liu et al., 2018). Substitution of key amino acids in enzymes is also an effective strategy for regulating grain shape. For example, two amino acid substitutions in the protein phosphatase GL3.1 reduce its activity and induce the production of longer grains (Hu et al., 2012). In this study we showed that SNP 27878401(T/A) in exon 3, which results in amino acid variation (Ser^{163}/Arg^{163}), affects the E3 ligase activity and ubiquitination level of GS3-2 (Figure 6), leading to variation in grain size.

In summary, CLG1 regulates grain size at two different levels. While a higher transcription level of the *CLG1* gene in the *clg1-1* mutant than in the wild type contributes to an increase in grain length, the fact that the natural isoform CLG1^{163S} has stronger E3 ligase activity than the isoform CLG1^{163R} also increases grain length. These effects may potentially be exploited for predictable design of grain shape in rice breeding.

METHODS

Plant materials and growth conditions

Rice (*Oryza sativa*) plants used in this study were grown in either a greenhouse under a short-day photoperiod (10-h day/14-h night) with a light intensity of 1.34 × 10 000 Lux at 30°C/25°C (day/night) or in a field located in Beijing under natural conditions. *O. sativa* L. ssp. *japonica* cv. Zhonghua 10 (ZH10) was used for transformation. Harvested grains were air dried, and the fully filled grains were used to measure grain length and width.

Vector construction and rice transformation

For generating the *CLG1* OEs, the full-length *CLG1* coding sequence was amplified by PCR and cloned into the *pCsVMV-HA3-N-1300* vector (Verdaguer et al., 1998) to generate the plasmid *CsVMV::CLG1*. To obtain mOE lines, the primers CLG1-mOE-F and CLG1-mOE-R (Supplemental Table 2) were used to amplify the mutated *CLG1* cDNA sequence according to a previous report (Barettino et al., 1994). The key residues for Zn^{2+} ion chelation in the RING domain, Cys^{713}, His^{715}, and His^{718}, were mutated into Ser^{713}, Tyr^{715}, and Tyr^{718}, respectively (Figure 1C), and the DNA fragment was cloned into *pCsVMV-HA3-N-1300* to generate plasmid *CsVMV::mCLG1*.

The knockout (KO) mutant lines were generated using CRISPR/Cas9. The sgRNAs target *CLG1* at location sg1, 5′-GCT TGA GGC TGA GAT ACG AA-3′. For KO genotyping, genomic DNA was extracted from transgenic plants and primer pairs flanking the designed target site were used for PCR amplification (Supplemental Table 2). Sequence alignment revealed that two different mutants, KO1 and KO2, were obtained (Figure 1D). For generating the mutants of *Os05g47770*, two target sites, 5′CAGCACCTTCGACTTCCC3′ and 5′CGCGCATATGGCGTCGTCG3′, were cloned into the pYLCRISPR-Cas9Pubi-H vector following the method described by a previous report (Ma et al., 2015).

The plasmids *CsVMV::CLG1*, *CsVMV::mCLG1*, and CRISPR/Cas9-sg1 were introduced into *A. tumefaciens* strain EHA105 and sent to Hangzhou Biogle for transformation into the ZH10 background.

The *Ubi::GS3-1:Flag* (GS3-1F) and *Ubi::GS3-4:Flag* (GS3-4F) transgenic plants were generated in our previous work (Sun et al., 2018).

RNA extraction and qRT–PCR

Plant total RNA was isolated using a TRIzol RNA extraction kit according to the user manual (15596, Invitrogen). Total RNA (2 μg) was used to synthesize cDNA using the High Capacity cDNA Reverse Transcription Kit (Thermo Fisher Scientific). The cDNA was diluted 1:30 into 15 μl SYBR Green Quantitative PCR Master Mix (QPK-201, Toyobo, Osaka, Japan), according to the manufacturer's instructions. qRT–PCR was performed on an Mx3000P instrument (Stratagene, La Jolla, CA, USA). Rice *UBIQUITIN* was used as an internal reference, and gene expression levels were normalized to the expression level of *UBIQUITIN*. Each experiment included three technical replicates with at least three biological replicates. The values represent means ± SE of three technical replicates.

Total RNA was extracted from young panicles (10 ± 1 cm in length) to detect the expression levels of 16 genes in a 128-kb region in the wild-type (ZH10) and mutant *CLG1-1* backgrounds. For determining the *CLG1* expression pattern in various organs, panicles, young leaves, flag leaves, and flowers were sampled for RNA extraction. For determining the transcription levels of genes in OE, mOE, CLG1-OE/GS3-1F, and CLG1-OE/GS3-4F transgenic plants, the 2-week-old seedlings of transgenic lines were used for RNA extraction. Primers used are listed in Supplemental Table 2.

RPSCCCNCNCNCCSSSSSSCGAALT**K**SPCR was ubiquitinated. The theoretical MW is 3659.35176, *z* is 4, and *m*/*z* = 915.5948. The carbamidomethyl modification occurred on each cysteine, and two glycines from ubiquitin were found on lysine in this peptide.

(D) GS3-1, but not G3-4, can be degraded through the endosome degradation pathway. Seedlings (approximately 2 weeks old) of *Ubi::GS3-1:Flag* and *Ubi::GS3-4:Flag* transgenic plants (Sun et al., 2018) were treated with CHX (an efficient inhibitor of eukaryotic protein synthesis) with or without E64d (an inhibitor of lysosomal/vacuolar hydrolases). The fusion proteins GS3-1:Flag and GS3-4:Flag were detected using an anti-Flag antibody. Rubisco was used as the internal control. The relative intensity is indicated above each band. Ponceau staining (lower panel) was done as a loading control.

(E) *In vivo* accumulation of GS3-1 and GS3-4 in *CLG1*-overexpressing plants. The protein levels of GS3-1:Flag and GS3-4:Flag were determined using an anti-Flag antibody. The number above each band indicates relative intensity. Ponceau staining (lower panel) was done as a loading control.

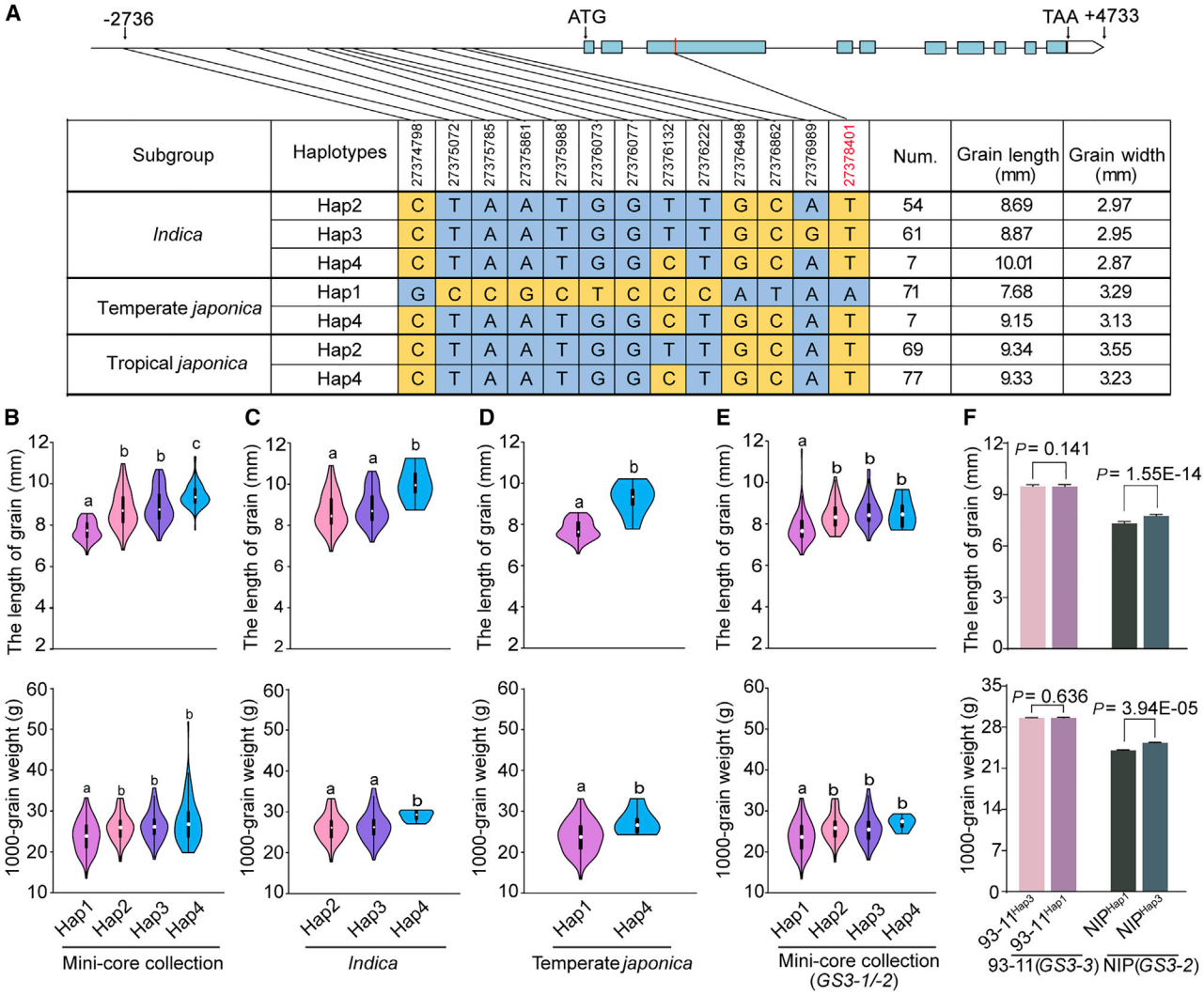

Subgroup	Haplotypes	27374798	27375072	27375785	27375861	27375988	27376073	27376077	27376132	27376222	27376498	27376862	27376989	27378401	Num.	Grain length (mm)	Grain width (mm)
Indica	Hap2	C	T	A	A	T	G	G	T	T	G	C	A	T	54	8.69	2.97
	Hap3	C	T	A	A	T	G	G	T	T	G	C	G	T	61	8.87	2.95
	Hap4	C	T	A	A	T	G	G	C	T	G	C	A	T	7	10.01	2.87
Temperate *japonica*	Hap1	G	C	C	G	C	T	C	C	C	A	T	A	A	71	7.68	3.29
	Hap4	C	T	A	A	T	G	G	C	T	G	C	A	T	7	9.15	3.13
Tropical *japonica*	Hap2	C	T	A	A	T	G	G	T	T	G	C	A	T	69	9.34	3.55
	Hap4	C	T	A	A	T	G	G	C	T	G	C	A	T	77	9.33	3.23

Figure 5. Natural variation of the *CLG1* gene and the effect on grain size.

(A) DNA polymorphisms in the *CLG1* locus among 346 cultivated accessions. The *CLG1* gene and SNPs are shown on the physical chromosome map based on the NIP sequence from MSU7 (rice.plantbiology.msu.edu). Num., number of accessions in each category.

(B–E) Boxplots of grain length and 1000-grain weight for 346 Asian cultivated rice accessions from the 3000 Rice Genome Project **(B)**, 122 *indica* accessions **(C)**, 78 temperate *japonica* accessions **(D)**, and 166 accessions with the *GS3-1* or *GS3-2* allele **(E)** carrying different *CLG1* haplotypes. Values are shown as means ± SEM (n = 60). The violin plot was constructed in R. Different letters indicate statistically significant differences between groups ($P < 0.05$), as determined by Tukey's honestly significant difference test.

(F) The effects of Hap1 and Hap3 of *CLG1* on grain length, grain width, and 1000-grain weight in the chromosome segment substitution lines (CSSLs) derived from the cross between 93-11 ($CLG1^{Hap3}$, *GS3-3*) and NIP ($CLG1^{Hap1}$, *GS3-2*). CSSL 93-11^{Hap1} carries a segment that includes $CLG1^{Hap1}$ from NIP in the 93-11 background, and CSSL NIP^{Hap3} carries $CLG1^{Hap3}$ from 93-11 in the NIP background. Values are shown as means ± SEM (n = 20). A Student's t-test was used to generate the P values.

Phylogenetic analysis

Homologous proteins used to construct phylogenetic trees were selected with the NCBI program (https://www.ncbi.nlm.nih.gov). ClustalW was used to align the amino acid sequences of selected proteins. Phylogenetic trees were generated using the neighbor-joining method in MEGA software version 7 (Kumar et al., 2016). Bootstrap values were from 1000 replicates.

In vivo ubiquitination assays

35S::Myc:GS3-1 and *35S::Myc:GS3-4* were expressed in *N. benthamiana* leaves. The ubiquitinated Myc:GS3-1 and Myc:GS3-4 proteins were immunoprecipitated by an anti-Myc antibody and detected with anti-ubiquitin antibodies (Zhang et al., 2015).

In vitro ubiquitination assays

The self-ubiquitination assays were performed largely as described previously (Xia et al., 2013). The coding sequence of *CLG1* was cloned into the *pMAL-C4X* vector to generate the fusion protein MBP:CLG1. For the *in vitro* self-ubiquitination assay, the fusion protein MBP:CLG1 was purified from the bacterial lysates of *E. coli* BL21 expressing MBP:CLG1. Then, about 0.5 μg MBP:CLG1 fusion protein or MBP was mixed with 100 ng E1 (Boston Biochem), 200 ng E2 (Boston Biochem), and 2 μg ubiquitin (Boston Biochem). Polyubiquitinated proteins were detected by immunoblotting with anti-ubiquitin antibody (ImmunoWay). To test whether CLG1 and mCLG1 ubiquitinated the substrate GS3, purified GST:GS3-1:Myc and GST:GS3-1:Myc were added at four-, two-, and one-fold molar in each reaction mixture; 4×, 2×, and 1× represent protein

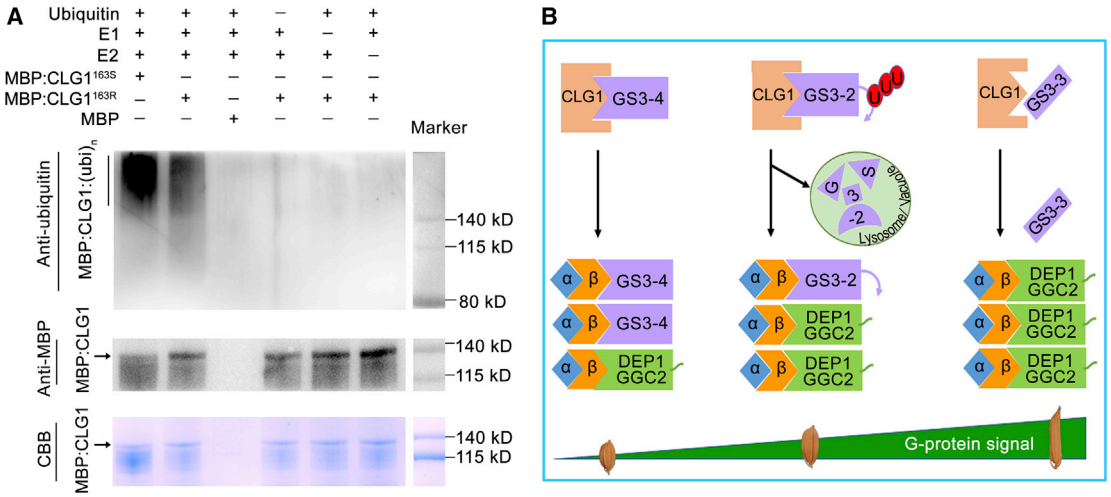

Figure 6. Comparison of the activity of CLG1^{163S} and CLG1^{163R} and a working model for the regulation of grain size by CLG1 and G-protein signaling.

(A) Self-ubiquitination assay of CLG1^{163S} and CLG1^{163R}. "+" and "−" denote the presence and absence, respectively, of the components in each reaction mixture. The gel stained with Coomassie brilliant blue (CBB) and western blotting using anti-MBP were used as loading controls.

(B) Working model for CLG1 and GS3. Both GS3-4 and GS3-2 can compete with DEP1 and GGC2 to bind to Gβ and regulate G-protein signaling. CLG1 interacts with and ubiquitinates the Gγ protein GS3-2, resulting in its degradation via the endosome-mediated pathway. Reduction of GS3-2 weakens its inhibition of G-protein signaling and leads to the production of long grains. The lack of a tail in GS3-4 prevents it from being degraded and results in the production of short grains.

contents of 0.4, 0.2, and 0.1 μg, respectively. The ubiquitinated GST:GS3-2:Myc and GST:GS3-4:Myc proteins were detected with anti-ubiquitin (ImmunoWay), anti-Myc antibody (CWBio), and anti-K63-linked-Ubiquitin (Abcam). MBP:CLG1 was detected with anti-MBP (New England Biolabs).

To compare the difference in E3 ligase activity between CLG1^{163R} and CLG1^{163S}, the coding sequences of *CLG1*^{163S} and *CLG1*^{163R} were individually cloned into the plasmid pMAL-C4X to allow expression of CLG1^{163S} or CLG1^{163R} as a fusion with MBP in *E. coli* strain BL21 (DE3). *In vitro* ubiquitination assays were performed as described above. Polyubiquitinated proteins were detected by immunoblotting with anti-ubiquitin antibody (ImmunoWay) and anti-MBP (New England Biolabs).

LC-MS analysis

Fusion protein GST:GS3-2 or GST:GS3-4 (0.5 μg) and fusion protein CLG1:MBP (0.5 μg) purified from *E. coli* BL21 were used. The reactions were performed with 100 ng E1 (Boston Biochem), 200 ng E2 (Boston Biochem), and 2 μg ubiquitin (Boston Biochem) in buffer containing 50 mM Tris (pH 7.4), 2 mM DTT, 5 mM $MgCl_2$, and 2 mM ATP. After incubation at 30°C for 2 h, the reaction products were separated on 4%–12% SDS–PAGE gels and stained with Coomassie brilliant blue. The bands representing ubiquitinated GST:GS3-2 and GST:GS3-4 were excised for LC-MS analysis according to the method described previously (van der Wal et al., 2018). NanoLC-MS mass spectra were acquired on an Oribtrap Tribrid Lumos mass spectrometer (Thermo) coupled to an EASY-nLC 1200 system (Thermo Fisher). Peptides were separated on an in-house packed 150 μM inner diameter column containing 15 cm Reprosil-pur 120 C18-AQ phase resin (1.9 μm, 120 Å, Dr. Maisch, Germany) with a gradient consisting of 2%–35% (80% AcN, 0.1% FA) over 90 min at 500 nl/min. For all experiments, the instrument was operated in the data-dependent acquisition mode. MS1 spectra were collected at a resolution of 120 000 with an automated gain control (AGC) target of 4E5 and a maximum injection time of 50 ms. Precursors were filtered according to charge state (2–7z), and monoisotopic peak assignment. Previously interrogated precursors were dynamically excluded for 30 s. Peptide precursors were isolated with a quadrupole mass filter set to a width of 1.6 Th. Ion trap MS2 spectra were collected at an AGC of 1E4, maximum injection time of 50 ms, and HCD collision energy of 32%.

For data analysis, RAW files were analyzed using the Proteome Discoverer software (version 2.2). The enzyme specificity was set to trypsin, with the maximum number of missed cleavages raised to three. Lysine with a diGly remnant, oxidation of methionine, and N-terminal acetylation were set as variable modifications. Carbamidomethylation of cysteine was set as a fixed modification. Searches were performed against a fasta file combined with Uniprot *E. coli* protein sequences and GS3-1, GS3-2, and GS3-4. Only peptides at a false discovery rate of 1% were accepted.

Y2H assays

Y2H analysis was performed using the MatchMaker GAL4 Two-Hybrid System 3 (Clontech) according to the manufacturer's manual. The full-length coding region of *CLG1* was cloned into the *pGADT7* vector as prey. The different coding regions of *GS3-2*, *GS3-4*, and sequences encoding various truncated GS3 proteins were individually ligated into *pGBKT7* to make the bait plasmid vectors. For the interaction test, each bait construct was co-transformed with each prey construct into the yeast strain AH109, plated on SD/-Trp-Leu medium, and grown at 30°C for 3 days. Then, co-transformed yeast clones were serially diluted (1:10, 1:100, 1:1000), and spotted and grown on SD/-Leu/-Trp/-His/-Ade medium at 30°C for 3 days. Empty vectors were co-transformed as negative controls. The primers used are listed in Supplemental Table 2.

Pull-down assay

To test the interaction between CLG1 and GS3, the open reading frame of *CLG1* was cloned into the *pGEX4T-1* vector to obtain GST:CLG1 fusion protein, and *GS3-2* was cloned into the plasmid *pMAL-C4X* to obtain MBP:GS3-2 fusion protein. Expression of the MBP:GS3-2 and GST:CLG1 fusion proteins and *in vitro* binding experiments were performed as described previously (Chen et al., 2013).

BiFC

For split luciferase complementation, *CLG1* and *GS3-2* were cloned into the vectors *pCM1300-nLUC* carrying the N-terminal half of luciferase and *pCM1300-cLUC* carrying the C-terminal half of luciferase,

respectively. cLUC and nLUC were used alone as controls following the protocol used for *N. benthamiana* leaves (You et al., 2016).

For BiFC assays in rice protoplasts, the coding sequences of *CLG1* and *GS3* were amplified and ligated into the *pUC-SPYNE* and *pUC-SPYCE* vectors, respectively (Walter et al., 2004). The plasmids were transformed into rice protoplasts that were obtained from leaf sheaths of 10-day-old etiolated seedlings using the polyethylene glycol-mediated transient expression system (Chen et al., 2006). The transformed protoplasts were observed using a fluorescence microscope (Olympus FV1000MPE). Images were analyzed with Image FV10-ASW 4.0 Viewer software.

Subcellular localization assay

To observe the localization of GS3-2 and GS3-4 with the early endosome marker OsSCAMP1 (*LOC_Os07g37740*), the coding sequences of *OsSCAMP1* and *GS3-2/GS3-4* were amplified and ligated into the *pCsVMV-mCherry-N-1300* and *pCAMBIA1301-GFP* vectors to generate *CsVMV::SCAMP1:mCherry* and *35S::GS3-2:GFP/35S::GS3-4:GFP*, respectively, following the previously described protocol for *N. benthamiana* leaves (Liu et al., 2010). Similarly, colocalization of GS3-2 and GS3-4 with the late endosome marker ARA7:mCherry (*At4g19640*) was observed according to a previous report (Yu et al., 2016). The fluorescence was visualized with a confocal scanning microscope (Olympus FV1000MPE) 48–72 h after infiltration.

To examine the dynamic distributions of GS3-2 and GS3-4, the plasmids *GS3-2:GFP* and *GS3-4:GFP*, respectively, were expressed in *N. benthamiana* leaves using agroinfiltration. The GFP fluorescence of GS3-2 and GS3-4 in the plasma membrane from 5 to 7 h after CHX treatment was observed, and the fluorescence intensity across the labeled area was determined using the ImageJ plot profile tool.

To validate the effect of mCLG1 on the endocytosis of GS3, GS3-2 was co-expressed with CLG1 or mCLG1 in *N. benthamiana* leaves using agroinfiltration, and the change in GS3 subcellular localization from 5 to 7 h after CHX treatment was examined. The fluorescence intensity of 20 points in the cytomembrane from 5 to 7 h after CHX treatment was determined using the ImageJ plot profile tool.

To confirm the trafficking of GS3-2 from the membrane to cytoplasm, GS3-2:GFP was co-expressed with the late endosome marker VPS23A:mCherry in *N. benthamiana* leaves using agroinfiltration. Treatment with the protein cargo transport inhibitor WM blocked protein cargo trafficking to lysosomes/vacuoles and resulted in the formation of enlarged multivesicular bodies.

Protein quantification in transgenic seedlings by western blot analysis

Seedlings (approximately 2 weeks old) of *Ubi::GS3-1:Flag* transgenic rice (GS3-1F) and *Ubi::GS3-4:Flag* transgenic rice (GS3-4F) were treated with CHX with or without E64d, an inhibitor of lysosomal/vacuolar hydrolases. Samples were collected at 0, 2, 4, and 6 h after treatment and lysed in extraction buffer (25 mM Tris–HCl [pH 7.5], 10 mM NaCl, 10 mM $MgCl_2$, 4 mM PMSF, 5 mM DTT, and 2 mM ATP) before centrifugation. The immunoprecipitates were electrophoretically separated on 12% SDS–PAGE gels and transferred to a polyvinylidene fluoride membrane. The fusion proteins GS3-1:Flag and GS3-4:Flag were detected by western blotting with anti-Flag antibody (Sigma catalog F3165, dilution 1:5000). The same method was used to detect fusion proteins GS3-1:Flag and GS3-4:Flag in CLG1-OE/GS3-1F and CLG1-OE/GS3-4F transgenic plants, respectively.

Haplotype analysis across the *CLG1* region

The haplotypes were constructed from SNPs (frequencies >5%) identified within a 7.7-kb region flanking CLG1 from 346 accessions of *O. sativa*. The Fastphase program (Scheet and Stephens, 2006) was used to fill in missing data to allow haplotype reconstruction across the target regions. Boxplots for grain length, width, and weight were generated using data from *indica* and *japonica* rice cultivars of Asian origin (346 accessions from the 3000 Rice Genome Project). The violin plot was constructed in R.

ACCESSION NUMBERS

All sequencing data generated in this study can be found in NCBI (https://www.ncbi.nlm.nih.gov)/MSU7 (rice.plantbiology.msu.edu)/RAP (The Rice Annotation Project, https://rapdb.dna.affrc.go.jp). *CLG1* (*Os05g47780*), *GS3* (*Os03g0407400*), *OsSCAMP1* (*Os07g37740*), *ARA7* (*At4g19640*), *VPS23A* (*At3g12400*), *GL3.1* (*Os03g44500*), *GSK2* (*Os05g11730*), *TGW6* (*Os06g41850*), *GS5* (*Os05g06660*), *GW5* (*DQ991205*).

SUPPLEMENTAL INFORMATION

Supplemental information can be found online at *Molecular Plant Online*.

FUNDING

This work was supported by grants from the National Key Research and Development Program (2016YFD0100901 and 2016YFD0100903) and the Earmarked Fund for the China Agricultural Research System (CARS-01-05).

AUTHOR CONTRIBUTIONS

K.C., Q.Z., and Y.X. conceived the project, supervised the study, and interpreted the data; W.Y. and Y.X. designed the experiments; W.Y. performed the experiments with assistance from B.W., S.G., H.L., X.G., and W.L.; W.Y. and Y.X. analyzed data with assistance from K.W., X.F., Y.O., and S.S.; W.Y., Y.X., and Q.Z. wrote the paper with assistance from K.C., X.F., and Y.O.

ACKNOWLEDGMENTS

We thank Dr. Zhuang Lu (the Plant Science Facility of the Institute of Botany, Chinese Academy of Science) for her excellent analysis of LC-MS data and Dr. Jingquan Li (the Plant Science Facility of the Institute of Botany, Chinese Academy of Science) for her technical assistance with the fluorescence microscope. No conflict of interest declared.

Received: June 10, 2021
Revised: June 26, 2021
Accepted: June 27, 2021
Published: June 30, 2021

REFERENCES

Aung, M.S., Kobayashi, T., Masuda, H., and Nishizawa, N.K. (2018). Rice HRZ ubiquitin ligases are crucial for response to excess iron. Physiol. Plantarum. **163**:282–296.

Barettino, D., Feigenbutz, M., Valcarcel, R., and Stunnenberg, H.G. (1994). Improved method for PCR-mediated site-directed mutagenesis. Nucleic Acids Res. **22**:541–542.

Botella, J.R. (2012). Can heterotrimeric G proteins help to feed the world? Trends Plant Sci. **17**:563–568.

Che, R.H., Tong, H.N., Shi, B.H., Liu, Y.Q., Fang, S.R., Liu, D.P., Xiao, Y.H., Hu, B., Liu, L.C., Wang, H.R., et al. (2015). Control of grain size and rice yield by GL2-mediated brassinosteroid responses. Nat. Plants **2**:15195.

Chen, S.B., Tao, L.Z., Zeng, L.R., Vega-Sanchez, M.E., Umemura, K., and Wang, G.L. (2006). A highly efficient transient protoplast system for analyzing defence gene expression and protein-protein interactions in rice. Mol. Plant Pathol. **7**:417–427.

Chen, Y., Xu, Y.Y., Luo, W., Li, W.X., Chen, N., Zhang, D.J., and Chong, K. (2013). The F-bBox protein OsFBK12 targets OsSAMS1 for degradation and affects pleiotropic phenotypes, including leaf senescence, in rice. Plant Physiol. **163**:1673–1685.

Choi, B.S., Kim, Y.J., Markkandan, K., Koo, Y.J., Song, J.T., and Seo, H.S. (2018). GW2 functions as an E3 ubiquitin ligase for rice expansin-lLike 1. Int. J. Mol. Sci. **19**:7.

Ding, S.C., Zhang, B., and Qin, F. (2015). *Arabidopsis* RZFP34/CHYR1, a ubiquitin E3 ligase, regulates stomatal movement and drought tolerance via SnRK2.6-mediated phosphorylation. Plant Cell **27**:3228–3244.

Dong, C.H., Agarwal, M., Zhang, Y.Y., Xie, Q., and Zhu, J.K. (2006). The negative regulator of plant cold responses, HOS1, is a RING E3 ligase that mediates the ubiquitination and degradation of ICE1. P. Natl. Acad. Sci. U S A. **103**:8281–8286.

Fan, C.C., Xing, Y.Z., Mao, H.L., Lu, T.T., Han, B., Xu, C.G., Li, X.H., and Zhang, Q.F. (2006). *GS3*, a major QTL for grain length and weight and minor QTL for grain width and thickness in rice, encodes a putative transmembrane protein. Theor. Appl. Genet. **112**:1164–1171.

Freemont, P.S., Hanson, I.M., and Trowsdale, J. (1991). A novel cysteine-rich sequence motif. Cell **64**:483–484.

Gao, T., Wu, Y.R., Zhang, Y.Y., Liu, L.J., Ning, Y.S., Wang, D.J., Tong, H.N., Chen, S.Y., Chu, C.C., and Xie, Q. (2011). *OsSDIR1* overexpression greatly improves drought tolerance in transgenic rice. Plant Mol. Biol. **76**:145–156.

Hao, J.Q., Wang, D.K., Wu, Y.B., Huang, K., Duan, P.G., Li, N., Xu, R., Zeng, D.L., Dong, G.J., Zhang, B.L., et al. (2021). The GW2-WG1-OsbZIP47 pathway controls grain size and weight in rice. Mol. Plant **14**:1–15.

Hicke, L., and Dunn, R. (2003). Regulation of membrane protein transport by ubiquitin and ubiquitin-binding proteins. Annu. Rev. Cell Dev. Biol. **19**:141–172.

Hu, J., Wang, Y.X., Fang, Y.X., Zeng, L.J., Xu, J., Yu, H.P., Shi, Z.Y., Pan, J.J., Zhang, D., Kang, S.J., et al. (2015). A rare allele of *GS2* enhances grain size and grain yield in rice. Mol. Plant **8**:1455–1465.

Hu, X.M., Qian, Q., Xu, T., Zhang, Y.E., Dong, G.J., Gao, T., Xie, Q., and Xue, Y.B. (2013). The U-bBox E3 ubiquitin ligase TUD1 functions with a heterotrimeric G alpha subunit to regulate brassinosteroid-mediated growth in rice. Plos Genet. **9**:e1003391.

Hu, Z.J., He, H.H., Zhang, S.Y., Sun, F., Xin, X.Y., Wang, W.X., Qian, X., Yang, J.S., and Luo, X.J. (2012). A kelch motif-containing serine/threonine protein phosphatase determines the large grain QTL trait in rice. J. Integr. Plant Biol. **54**:979–990.

Huang, K., Wang, D.K., Duan, P.G., Zhang, B.L., Xu, R., Li, N., and Li, Y.H. (2017). *WIDE AND THICK GRAIN 1*, which encodes an otubain-like protease with deubiquitination activity, influences grain size and shape in rice. Plant J. **91**:849–860.

Huang, X.Z., Qian, Q., Liu, Z.B., Sun, H.Y., He, S.Y., Luo, D., Xia, G.M., Chu, C.C., Li, J.Y., and Fu, X.D. (2009). Natural variation at the *DEP1* locus enhances grain yield in rice. Nat. Genet. **41**:494–497.

Ishimaru, K., Hirotsu, N., Madoka, Y., Murakami, N., Hara, N., Onodera, H., Kashiwagi, T., Ujiie, K., Shimizu, B., Onishi, A., et al. (2013). Loss of function of the IAA-glucose hydrolase gene *TGW6* enhances rice grain weight and increases yield. Nat. Genet. **45**:707–711.

Jung, C., Zhao, P.Z., Seo, J.S., Mitsuda, N., Deng, S.L., and Chua, N.H. (2015). PLANT U-BOX PROTEIN10 regulates MYC2 stability in *Arabidopsis*. Plant Cell **27**:2016–2031.

Kobayashi, T., Nagasaka, S., Senoura, T., Itai, R.N., Nakanishi, H., and Nishizawa, N.K. (2013). Iron-binding haemerythrin RING ubiquitin ligases regulate plant iron responses and accumulation. Nat. Commun. **4**:2792.

Koiwai, H., Tagiri, A., Katoh, S., Katoh, E., Ichikawa, H., Minami, E., and Nishizawa, Y. (2007). RING-H2 type ubiquitin ligase EL5 is involved in root development through the maintenance of cell viability in rice. Plant J. **51**:92–104.

Kumar, S., Stecher, G., and Tamura, K. (2016). MEGA7: molecular evolutionary genetics analysis version 7.0 for bigger datasets. Mol. Biol. Evol. **33**:1870–1874.

Lam, S.K., Siu, C.L., Hillmer, S., Jang, S., An, G.H., Robinson, D.G., and Jiang, L.W. (2007). Rice SCAMP1 defines clathrin-coated, trans-Golgi-located tubular-vesicular structures as an early endosome in tobacco BY-2 cells. Plant Cell **19**:296–319.

Lauwers, E., Jacob, C., and Andre, B. (2009). K63-linked ubiquitin chains as a specific signal for protein sorting into the multivesicular body pathway. J. Cell Biol. **185**:493–502.

Li, Y.H., Zheng, L.Y., Corke, F., Smith, C., and Bevan, M.W. (2008). Control of final seed and organ size by the DA1 gene family in *Arabidopsis thaliana*. Genes Dev. **22**:1331–1336.

Lim, S.D., Jung, C.G., Park, Y.C., Lee, S.C., Lee, C., Lim, C.W., Kim, D.S., and Jang, C.S. (2015). Molecular dissection of a rice microtubule-associated RING finger protein and its potential role in salt tolerance in *Arabidopsis*. Plant Mol. Biol. **89**:365–384.

Liu, J.F., Chen, J., Zheng, X.M., Wu, F.Q., Lin, Q.B., Heng, Y.Q., Tian, P., Cheng, Z.J., Yu, X.W., Zhou, K.N., et al. (2017). *GW5* acts in the brassinosteroid signalling pathway to regulate grain width and weight in rice. Nat. Plants. **3**:17043.

Liu, J.P., Zhang, C.C., Wei, C.C., Liu, X., Wang, M.G., Yu, F.F., Xie, Q., and Tu, J.M. (2016). The RING finger ubiquitin E3 ligase OsHTAS enhances heat tolerance by promoting H_2O_2-induced stomatal closure in rice. Plant Physiol. **170**:429–443.

Liu, L.J., Zhang, Y.Y., Tang, S.Y., Zhao, Q.Z., Zhang, Z.H., Zhang, H.W., Dong, L., Guo, H.S., and Xie, Q. (2010). An efficient system to detect protein ubiquitination by agroinfiltration in *Nicotiana benthamiana*. Plant J. **61**:893–903.

Liu, Q., Han, R.X., Wu, K., Zhang, J.Q., Ye, Y.F., Wang, S.S., Chen, J.F., Pan, Y.J., Li, Q., Xu, X.P., et al. (2018). G-protein beta gamma subunits determine grain size through interaction with MADS-domain transcription factors in rice. Nat. Commun. **9**:852.

Ma, X.L., Zhang, Q.Y., Zhu, Q.L., Liu, W., Chen, Y., Qiu, R., Wang, B., Yang, Z.F., Li, H.Y., Lin, Y.R., et al. (2015). A robust CRISPR/Cas9 system for convenient, high-efficiency multiplex genome editing in monocot and dicot plants. Mol. Plant **8**:1274–1284.

Mao, H.L., Sun, S.Y., Yao, J.L., Wang, C.R., Yu, S.B., Xu, C.G., Li, X.H., and Zhang, Q.F. (2010). Linking differential domain functions of the GS3 protein to natural variation of grain size in rice. P. Natl. Acad. Sci. U S A. **107**:19579–19584.

Morreale, F.E., and Walden, H. (2016). SnapShot: types of ubiquitin ligases. Cell **165**:248.e1.

Park, C.H., Chen, S.B., Shirsekar, G., Zhou, B., Khang, C.H., Songkumarn, P., Afzal, A.J., Ning, Y.S., Wang, R.Y., Bellizzi, M., et al. (2012). The magnaporthe oryzae effector AvrPiz-t targets the RING E3 ubiquitin ligase APIP6 to suppress pathogen-associated molecular pattern-triggered immunity in rice. Plant Cell **24**:4748–4762.

Peng, Y.J., Shih, C.F., Yang, J.Y., Tan, C.M., Hsu, W.H., Huang, Y.P., Liao, P.C., and Yang, C.H. (2013). A RING-type E3 ligase controls anther dehiscence by activating the jasmonate biosynthetic pathway gene DEFECTIVE IN ANTHER DEHISCENCE1 in *Arabidopsis*. Plant J. **74**:310–327.

Qi, P., Lin, Y.S., Song, X.J., Shen, J.B., Huang, W., Shan, J.X., Zhu, M.Z., Jiang, L.W., Gao, J.P., and Lin, H.X. (2012). The novel quantitative trait locus *GL3.1* controls rice grain size and yield by regulating Cyclin-T1;3. Cell Res **22**:1666–1680.

Qiu, W.R., Xu, C.H., Xiao, X., and Xu, D. (2019). Computational prediction of ubiquitination proteins using evolutionary profiles and functional domain annotation. Curr. Genomics. **20**:389–399.

Raiborg, C., and Stenmark, H. (2009). The ESCRT machinery in endosomal sorting of ubiquitylated membrane proteins. Nature **458**:445–452.

Robinson, D.G., Jiang, L.W., and Schumacher, K. (2008). The endosomal system of plants: charting new and familiar territories. Plant Physiol. **147**:1482–1492.

Ruan, B.P., Shang, L.G., Zhang, B., Hu, J., Wang, Y.X., Lin, H., Zhang, A.P., Liu, C.L., Peng, Y.L., Zhu, L., et al. (2020). Natural variation in the promoter of *TGW2* determines grain width and weight in rice. New Phytol. **227**:629–640.

Scheet, P., and Stephens, M. (2006). A fast and flexible statistical model for large-scale population genotype data: applications to inferring missing genotypes and haplotypic phase. Am. J. Hum. Genet. **78**:629–644.

Selote, D., Matthiadis, A., Gillikin, J.W., Sato, M.H., and Long, T.A. (2018). The E3 ligase BRUTUS facilitates degradation of VOZ1/2 transcription factors. Plant Cell Environ **41**:2463–2474.

Selote, D., Samira, R., Matthiadis, A., Gillikin, J.W., and Long, T.A. (2015). Iron-binding E3 ligase mediates iron response in plants by targeting basic helix-loop-helix transcription factors. Plant Physiol. **167**:273–286.

Spitzer, C., Schellmann, S., Sabovljevic, A., Shahriari, M., Keshavaiah, C., Bechtold, N., Herzog, M., Muller, S., Hanisch, F.G., and Hulskamp, M. (2006). The *Arabidopsis elch* mutant reveals functions of an ESCRT component in cytokinesis. Development **133**:4679–4689.

Song, X.J., Huang, W., Shi, M., Zhu, M.Z., and Lin, H.X. (2007). A QTL for rice grain width and weight encodes a previously unknown RING-type E3 ubiquitin ligase. Nat. Genet. **39**:623–630.

Stone, S.L., Hauksdottir, H., Troy, A., Herschleb, J., Kraft, E., and Callis, J. (2005). Functional analysis of the RING-type ubiquitin ligase family of *Arabidopsis*. Plant Physiol. **137**:13–30.

Sun, S.Y., Wang, L., Mao, H.L., Shao, L., Li, X.H., Xiao, J.H., Ouyang, Y.D., and Zhang, Q.F. (2018). A G-protein pathway determines grain size in rice. Nat. Commun. **9**:851.

van der Wal, L., Berstarosti, K., Sap, K.A., Dekkers, D.H.W., Rijkers, E., Mientjes, E., Elgersma, Y., and Demmers, J.A.A. (2018). Improvement of ubiquitylation site detection by Orbitrap mass spectrometry. J. Proteomics **172**:49–56.

Verdaguer, B., de Kochko, A., Fux, C.I., Beachy, R.N., and Fauquet, C. (1998). Functional organization of the cassava vein mosaic virus (CsVMV) promoter. Plant Mol. Biol. **37**:1055–1067.

Walter, M., Chaban, C., Schütze, K., Batistic, O., Weckerman, K., and Näke, C. (2004). Visualization of protein interactions in living plant cells using bimolecular fluorescence complementation. Plant J. **40**:428–438.

Wang, S.S., Wu, K., Qian, Q., Liu, Q., Li, Q., Pan, Y.J., Ye, Y.F., Liu, X.Y., Wang, J., Zhang, J.Q., et al. (2017). Non-canonical regulation of SPL transcription factors by a human OTUB1-like deubiquitinase defines a new plant type rice associated with higher grain yield. Cell Res **27**:1142–1156.

Wang, S.K., Wu, K., Yuan, Q.B., Liu, X.Y., Liu, Z.B., Lin, X.Y., Zeng, R.Z., Zhu, H.T., Dong, G.J., Qian, Q., et al. (2012). Control of grain size, shape and quality by *OsSPL16* in rice. Nat. Genet. **44**:950–954.

Wang, S.K., Li, S., Liu, Q., Wu, K., Zhang, J.Q., Wang, S.S., Wang, Y., Chen, X.B., Zhang, Y., Gao, C.X., et al. (2015a). The *OsSPL16-GW7* regulatory module determines grain shape and simultaneously improves rice yield and grain quality. Nat. Genet. **47**:949–954.

Wang, Y.X., Xiong, G.S., Hu, J., Jiang, L., Yu, H., Xu, J., Fang, Y.X., Zeng, L.J., Xu, E.B., Xu, J., et al. (2015b). Copy number variation at the *GL7* locus contributes to grain size diversity in rice. Nat. Genet. **47**:944–948.

Weng, J.F., Gu, S.H., Wan, X.Y., Gao, H., Guo, T., Su, N., Lei, C.L., Zhang, X., Cheng, Z.J., Guo, X.P., et al. (2008). Isolation and initial characterization of *GW5*, a major QTL associated with rice grain width and weight. Cell Res **18**:1199–1209.

Xia, D., Zhou, H., Liu, R.J., Dan, W.H., Li, P.B., Wu, B., Chen, J.X., Wang, L.Q., Gao, G.J., Zhang, Q.L., et al. (2018). *GL3.3*, a novel QTL encoding a GSK3/SHAGGY-like kinase, epistatically interacts with GS3 to produce extra-long grains in rice. Mol. Plant **11**:754–756.

Xia, T., Li, N., Dumenil, J., Li, J., Kamenski, A., Bevan, M.W., Gao, F., and Li, Y.H. (2013). The ubiquitin receptor DA1 interacts with the E3 ubiquitin ligase DA2 to regulate seed and organ size in *Arabidopsis*. Plant Cell **25**:3347–3359.

Xie, Q., Guo, H.S., Dallman, G., Fang, S.Y., Weissman, A.M., and Chua, N.H. (2002). SINAT5 promotes ubiquitin-related degradation of NAC1 to attenuate auxin signals. Nature **419**:167–170.

Xu, C.J., Liu, Y., Li, Y.B., Xu, X.D., Xu, C.G., Li, X.H., Xiao, J.H., and Zhang, Q.F. (2015). Differential expression of *GS5* regulates grain size in rice. J. Exp. Bot. **66**:2611–2623.

Xu, Q., Zhao, M.Z., Wu, K., Fu, X.D., and Liu, Q. (2016). Emerging insights into heterotrimeric G protein signaling in plants. J. Genet. Genomics. **43**:495–502.

Xu, R., Li, N., and Li, Y.H. (2019). Control of grain size by G protein signaling in rice. J. Integr. Plant Biol. **61**:533–540.

Yang, L., Liu, Q.H., Liu, Z.B., Yang, H., Wang, J.M., Li, X.F., and Yang, Y. (2016). *Arabidopsis* C3HC4-RING finger E3 ubiquitin ligase AtAIRP4 positively regulates stress-responsive abscisic acid signaling. J. Integr. Plant Biol. **58**:67–80.

Yang, Y., Fu, D.B., Zhu, C.M., He, Y.Z., Zhang, H.J., Liu, T., Li, X.H., and Wu, C.Y. (2015). The RING-hinger ubiquitin ligase HAF1 mediates heading date 1 degradation during photoperiodic flowering in rice. Plant Cell **27**:2455–2468.

You, Q.Y., Zhai, K.R., Yang, D.L., Yang, W.B., Wu, J.N., Liu, J.Z., Pan, W.B., Wang, J.J., Zhu, X.D., Jian, Y.K., et al. (2016). An E3 ubiquitin ligase-BAG protein module controls plant innate immunity and broad-spectrum disease resistance. Cell Host Microbe **20**:758–769.

Yu, F., Lou, L., Tian, M., Li, Q., Ding, Y., Cao, X., Wu, Y., Belda-Palazon, B., Rodriguez, P.L., Yang, S., et al. (2016). ESCRT-I component VPS23A affects ABA signaling by recognizing ABA receptors for endosomal degradation. Mol. Plant **9**:1570–1582.

Zhang, X.J., Wang, J.F., Huang, J., Lan, H.X., Wang, C.L., Yin, C.F., Wu, Y.Y., Tang, H.J., Qian, Q., Li, J.Y., et al. (2012). Rare allele of *OsPPKL1* associated with grain length causes extra-large grain and a significant yield increase in rice. P. Natl. Acad. Sci. U S A. **109**:21534–21539.

Zhang, H.W., Cui, F., Wu, Y.R., Lou, L.J., Liu, L.J., Tian, M.M., Ning, Y.S., Shu, K., Tang, S.Y., and Xie, Q. (2015). The RING finger ubiquitin E3 ligase SDIR1 targets SDIR1-INTERACTING PROTEIN1 for degradation to modulate the salt stress response and ABA signaling in *Arabidopsis*. Plant Cell **27**:214–227.

Zhang, X.R., Garreton, V., and Chua, N.H. (2005). The AIP2 E3 ligase acts as a novel negative regulator of ABA signaling by promoting ABI3 degradation. Gene Dev. **19**:1532–1543.

Zhang, Y.Y., Yang, C.W., Li, Y., Zheng, N.Y., Chen, H., Zhao, Q.Z., Gao, T., Guo, H.S., and Xie, Q. (2007). SDIR1 is a RING finger E3 ligase that positively regulates stress-responsive abscisic acid signaling in *Arabidopsis*. Plant Cell **19**:1912–1929.